Scientific Research Publishing

Open Journal of Radiology, 2022, 12, 125-141
https://www.scirp.org/journal/ojrad
ISSN Online: 2164-3032
ISSN Print: 2164-3024

Simulating Medical Imaging X-Ray Tubes with Various Parameters Using BEAMnrc Monte Carlo Software

Nikolaos Chatzisavvas[1*], Thanasis Koustas[2], Georgios Karpetas[3], Ioannis Valais[4], Georgios Priniotakis[1], Dimitrios Nikolopoulos[1]

[1]Department of Industrial Design and Production Engineering, University of West Attica, Athens, Greece
[2]Department of Medical Physics, Medical School, University of Patras, Patra, Greece
[3]Medical School, University of Thessaly, Larissa, Greece
[4]Department of Biomedical Engineering, University of West Attica, Athens, Greece
Email: *nchatzisavvas@uniwa.gr

How to cite this paper: Chatzisavvas, N., Koustas, T., Karpetas, G., Valais, I., Priniotakis, G. and Nikolopoulos, D. (2022) Simulating Medical Imaging X-Ray Tubes with Various Parameters Using BEAMnrc Monte Carlo Software. *Open Journal of Radiology*, **12**, 125-141.
https://doi.org/10.4236/ojrad.2022.123014

Received: August 24, 2022
Accepted: September 25, 2022
Published: September 28, 2022

Abstract

Context: Medical imaging has a wide range of applications in today's society. Basic projectional radiography, CT scans, mammograms and a range of other advanced technologies all use x-rays to create a large number of examinations every day across the world. The most essential component of such medical equipment is the x-ray tube, which creates and produces x-rays. **Objective:** We describe and investigate an abstract model-geometry of a simple x-ray tube utilizing the open-source software package of BEAMnrc of the EGSnrcmp family, which is well validated by several studies over the years, for high and low energy photons generation. **Methodology:** Our research focuses on two different electron beam energies: 120 keV and 30 keV. The 120 keV is the typical energy for simple projectional radiographic exams and CT examinations, whereas the 30 keV is the typical energy of mammography. **Results:** Two different anode materials are used for each case, Gold (Au) and Tungsten (W) for 120 keV because these are the most common in projectional radiography and CT; Molybdenum (Mo) and Rhodium (Rh) for 30 keV because with these targets most mammography exams are carried out. The aim of this work is to show how the BEAMnrc software package can simulate effectively x-ray generation of low-energy photons which are utilized in modern medical imaging procedures. We describe useful information on anode-target characteristics, such as anode angle, anode material, and metal filter materials, based on previous quality studies even by using software other than BEAMnrc. **Conclusion:** We demonstrate that BEAMnrc can be efficiently used for Monte Carlo modeling of low-energy photons.

Keywords

Bremsstrahlung, Filter, Monte Carlo, Spectral Distribution, X-Ray Tube

1. Introduction

The spectrum distribution of photons produced by an x-ray tube is crucial for various medical operations, along with CT medical imaging [1], dosimetry [2], x-ray fluorescence [3], mammography [4], dental radiography [5], radiotherapy [6], and so on. The aim of our work is to analyze the x-ray tube photon production using BEAMnrc Monte Carlo software, because several other studies have been completed using other software as e.g., MCNP [7], GEANT4 [8].

The scope is to identify crucial parameters such as anode target materials [2], anode angles [7] and filtration materials [9] which, in combination with existing research with other Monte Carlo software packages, will allow us to determine a Medical Imaging tube-standard which can be utilized by other EGSnrc users providing, simultaneously, tube information not easily accessible. This is very important, because manufacturers and vendors do not provide construction and spectrum data for x-ray tubes at photon energies of 120 keV and 30 keV, making it, hence, difficult to uncover such characteristics.

Our intention is to demonstrate that BEAMnrc is capable in mimicking x-ray creation at low energies as good as other commercial software, with the benefit of its free distribution, capabilities and independent multilayers design.

Electrons emitted from a filament due to thermionic emission, in a vacuum tube are driven at high velocity and bombard an anode-target. Tungsten and gold are typically employed as target materials in medical imaging x-ray tubes because of properties such as their high atomic mass and melting point, which are significant for CT and basic radiography at energies between 80 - 150 keV [10].

The target-anode materials at energies between 10 - 30 keV, where most mammographic exams are conducted, employ mainly molybdenum and rhodium as target materials. A heated filament generates electrons, which are subsequently converted to x-ray photons through the emission of Bremsstrahlung and the creation of characteristic x-rays [11]. The anode's inclination affects x-ray consumption inside the target and, thus, when the angle is increased, a higher number of photons can mix with primary beam as the anode's self-consumption diminishes [12] [13].

To decrease radiation exposure, x-rays are created inside the anode material and various high Z-materials are employed as filters [14] [15]. Aluminium and copper are mostly used at energies of 80 - 150 keV because these preferentially filter out the low energy photons that contribute to the skin's radiation exposure while, simultaneously, retain excellent picture contrast for clinical analysis. Because the energies in mammography are low, around 10 - 30 keV, and subse-

quently mammography has a potential of radiation damage and cancer [16], the use of filtration is extremely important. The most suitable metals that can be used as filters between 10 - 30 keV, are rhodium and molybdenum.

Even in complicated geometries, the Monte Carlo approach for simulating particle passage through matter, is the most precise method for x-ray spectrum production [17] [18] [19]. The transportation of electrons and photons within the target and filters, can be estimated by utilizing the Monte Carlo approach, through which, extensive information can be calculated regarding the components that contribute to the creation of the x-ray spectrum. BEAMnrc [20] [21] [22] [23], a part of the EGSnrcmp application code, is frequently used to simulate megavoltage clinical linear accelerators. However, via modifications and use of EGSnrcmp-layer modules, it can be used for simulating the generation of lower energy x-ray tubes, as effectively. Due to this, it is chosen as the appropriate code for this investigation. X-ray tube simulations utilizing the Monte Carlo approach have a significant cost in computational time, especially, when many bremsstrahlung photons are created by electrons in the keV energy range.

When running such simulations, the smallest decrease in calculation speed is crucial. The directional bremsstrahlung splitting approach is utilized in our procedures to reduce variance [24]. The necessity of applying variance reduction techniques to drastically reduce simulation time is emphasized. Very significant is also the investigation of the impact of the target's angle in the spectra on all of the scenarios that we've chosen. Finally, it is illustrated how the various metals that act as filters, and, are placed right after the x-ray tube, can affect the spectral distributions.

After conducting research, we have managed to detect, the specifications of various materials that are used anodes, the operational angles of each employed tube and the utilized filtering materials. We wanted to examine x-ray tubes for CT, basic radiography and mammography, two distinct energies, e.g., 120 keV and 30 keV are chosen for that purpose. In each energy, two different materials for the anode are employed. The number of photons generated with and without variance reduction technique is calculated, showing how much computational time can be saved. Also as per previous studies it is shown that as the angle of the x-ray tube increases, the number of scored photons increases due to the anode's self-absorption. Lastly, it is shown that in modern x-ray tube used for diagnostic purposes the use of filter reduces the low-energy bremsstrahlung photons that do not participate in the diagnostic process, lowering, hence, the dose in an examination. Various researchers [12] [13] chose other software for their Monte Carlo simulations and determine that the angle, anode material and filtration. These parameters play a very important role and needs to be studied further, in order to create more efficient x-rays tubes to use them in our everyday medical applications. It is hard to find via experimentation what is the best operational angle, the effect of operational angle in x-ray spectra, what are the suitable target materials and filter materials and what are the best combinations

we can determine for the x-ray tube to operate and in what application, e.g. CT, dental radiology, mammography etc. That is the reason Monte Carlo can help us identify such parameters.

We contribute to the field through the open-source program BEAMnrc, which may be further used to conduct simulated experiments of modern x-ray tubes.

2. Materials and Methods

Modern medical imaging x-ray tube design has offered novel solutions to difficulties like rotating anode targets, improved circuit design, that provide power to the filament and anode-cathode circuits, improved tube housing, for more radiation shielding, etc. [25]. The method that we utilize focuses mostly on the creation of x-rays using various materials and characteristics within the production module, which for the BEAMnrc's case, is the XTUBE module. The operational default values for each case (CT and mammography) are W-Au target materials, 22˚ operational angle and thin layers of 0.25 cm Al - 0.25 cm Al + 0.02 cm Cu to act as filters for the CT operation and 0.003 cm Mo - 0.003 cm Rh target materials, 17˚ operational angle and thin layers of Mo-Rh to act as filters. The above values were determined from past works and we chose these values as the research of x-ray tubes has been progressed over the years.

We are modelling a monoenergetic beam of electrons striking the anode at 120 keV and 30 keV respectively, simulating high quality DC voltage. Since x-ray tube filament-cathode relation is a computerized procedure that generates a single photon at the beginning of each Monte Carlo run, it is important to pre-determine the total number of runs, *i.e.*, the total number of Monte Carlo generated x-ray photons. Towards this, we generate 40 million electron particles for the 120 keV tube and 400 million for the 30 keV tube. The anode-target materials of tungsten and gold with filters of aluminium and copper, at angles of 17˚, 22˚, 27˚ degrees [12] are modelled for the 120 keV x-ray tube [13]. For the 30 keV case, x-ray tube target materials are molybdenum and rhodium, with filters of rhodium and molybdenum [8], at angles of 12˚, 17˚, 22˚ degrees [13].

The energy transfer thresholds AE and AP are set at 512 keV and 1 keV, respectively, while the cut-off energies ECUT and PCUT are set to 660 keV and 150 keV. Because the utilized geometry is the x-ray tube component, we employ the BEAMnrc GUI environment's components XTUBE and SLABS to describe our geometry. Then, several rectangular components are employed with varying thicknesses to configure the filters and the scoring plane. The thickness of the anode-target is set to 1 cm in the Z direction, underneath the XTUBE component we specify a 20 cm × 20 cm vacuum rectangle with 2 cm thickness on the Z axis, followed by a 20 cm × 20 cm air gap with 2 cm thickness on the Z axis, and finally, a 20 cm × 20 cm rectangle with the filters. Note that the thicknesses of the filters depend on the scenario we are exaggerating. We set the materials of the filters to air in the cases where filtering is air. Underneath the final slab

component, the scoring plane is placed.

The world's medium is set to AIR, the material in front of the XTUBE component and on the back is set to vacuum. The combination of materials for the target-anode, (W, Au, Mo, Rh) and the filters (Al, Al + Cu, Mo, Rh) [26] [27] can be found in Table 1. For some runs, we use the variance reduction technique and the exact same runs take place altering just the option of variance reduction to off. The corresponding results can be found in Table 2. The importance of the variance reduction technique (DBS) can be observed. It is very significant that the total simulation time is reduced, while, importantly, more particles hit and score in our phase space files.

Table 1. Target-anode, filter materials and target-anode angle combinations.

Anode Material/x-ray tube angle	Electron Beam Energy	Filter Material
W/22˚	120 keV	AIR
W/22˚	120 keV	0.25 cm AL
W/22˚	120 keV	0.25 cm AL + 0.02 cm Cu
W/17˚	120 keV	AIR
W/27˚	120 keV	AIR
Au/22˚	120 keV	AIR
Au/22˚	120 keV	0.25 cm AL
Au/22˚	120 keV	0.25 cm AL + 0.02 cm Cu
Au/17˚	120 keV	AIR
Au/27˚	120 keV	AIR
Mo/17˚	30 keV	AIR
Mo/17˚	30 keV	0.003 cm Mo
Mo/17˚	30 keV	0.003 cm Rh
Mo/12˚	30 keV	AIR
Mo/22˚	30 keV	AIR
Rh/17˚	30 keV	AIR
Rh/17˚	30 keV	0.003 cm Rh
Rh/17˚	30 keV	0.003 cm Mo
Rh/12˚	30 keV	AIR
Rh/22˚	30 keV	AIR

Table 2. Target-anode materials with and without DBS variance reduction technique.

Anode Material/ x-ray tube angle	Initial Particles	Scored Particles		Scored Photons	
		No DBS	With DBS	No DBS	With DBS
W/22˚	40,000,000	8,885,024	188,712,112	204,752	179,989,224
Au/22˚	40,000,000	16,165,648	197,585,432	401,316	196,550,620
Mo/17˚	400,000,000	298,895	266,714,288	298,790	266,598,226
Rh/17˚	400,000,000	286,663	255,775,360	286,661	255,666,429

The EGSnrc parameters that we use throughout this study are as follows. The algorithm EXACT is used for crossing the boundaries, the method PRESTA-II for the step of each electron particle, option on for the effects of the spin of the electron, the Koch-Motz distribution is utilized for the bremsstrahlung angular sampling (*i.e.* calculation of the emission angles of bremsstrahlung photons), the NRC cross sections database for bremsstrahlung is selected, bound Compton scattering is enabled, Koch-Motz pair angular sampling is selected, the pair cross sections of the NRC database are utilized, the sampling for angular photoelectrons is turned on, we take into account the scattering due to the Rayleigh phenomena, we account the atomic relaxations by switching the corresponding option to on and the photon cross-sections of the xcom database are chosen. The type of electron beam source is the parallel circular beam, *i.e.*, 90 degrees' incident angle between X-Y axis and zero angle between both X-Z and Y-Z axes. The beam source radius is set to 0.02 cm and the kinetic energy is 120 keV and 30 keV, as aforementioned. The value was chosen so that the focal spot of the beam produced to be the default option for the two energy cases. Over the year's other research has been conducted for various sources for medical imaging examination [28], as for our research we are more focused on the typical model of the bombardment of high velocity electrons on a metal target and the production of characteristic x-rays.

The phase space files produced were from 2.2 Gigabytes to 7.5 Gigabytes based on the filtration substance and initial kinetic energies of the electrons. For the combination of x-ray tube at 120 keV electron beam energy, 40×10^6 electron particles were initially produced by the cathode towards the anode-target, and, for the 30 keV, 40×10^7 electron particles were used. Depending on the filters and the starting particles, each simulation took around 8 - 12 hours to complete so as to minimize the uncertainties. From all our phase space files we extract information using BEAMDP [29] application and present the generated spectral distributions via xmgrace software [30].

3. Results and Discussions

Our study is being divided into four processes, the first process is to measure the effect that the usage of directional bremsstrahlung splitting variance reduction technique has on the data and the calculation time. The second process is to validate our simulations of the four different anode-target materials used and evaluate the Spectral distributions produced with the theoretical x-ray characteristics of the materials. The third process is to evaluate the affect that the anode angle has on the Spectral distributions. The fourth and last process is to show the effect of filtering the x-rays produced on the x-ray spectra.

Firstly, we would like to emphasize to the negative effect that the lack of variance reduction techniques imposes. This is characteristically shown in **Table 2**, where the initial particles generate significantly lower scored particles both for the simulation of the materials Mo and Rh at 30 keV incident energy and the

materials W and Au at 120 keV. It should be noted from Table 2, that the initial particles for materials W and Au are one order higher (40×10^7) compared to the ones of Mo and Rh materials. This was implemented because, for low energy x-ray beams, the bremsstrahlung phenomena in the electron beam hitting the anode, are significantly less probable and, in this manner, much more initial electrons are needed for the effective modelling of the bombardment of the anode-target material which generates the x-rays. The size of the phase space files was improved by using the DBS (Directional Bremsstrahlung Splitting) variance reduction technique, which also enables the much faster code execution and outcome scoring. For each case, we can clearly see that the scored particles and photons are increased by 2 - 3 orders of magnitude while, importantly, reducing the simulation by 20 - 30 times.

Next the approach of employing AIR as a filter is shown. In this way, the scored photons are simulated as being directly generated from the anode, at 22˚ for the 120 keV tube and at 17˚ for the 30 keV tube, as also, Adeli *et al. [8]* have implemented. However, in this publication the MCNP and Geant4 Monte Carlo software were used. As can be observed the BEAMnrc produce results comparable to MCNP and Geant4, for all anode-target materials and that is a very important finding. It implies, clearly, that the present model, the coding and the simulation are adequate and can be considered valid. The reader should emphasize here that both EGSnrcmp and BEAMnrc are codes well validated both for the high photon energy range and, most importantly, the low energy one [23] [24].

In Tables 3-6, the values of x-ray characteristic radiation for the Tungsten (W), Gold (Au), Molybdenum (Mo) and Rhodium (Rh) anode-target are presented from publication of Thomson *et al.* [31]. In Figures 1-4 the Spectral Distributions

Table 3. Tungsten (W) x-ray characteristic [31].

Material	K_{a1} (MeV)	K_{a2} (MeV)	K_{b1} (MeV)	K_{b2} (MeV)	$L_{a,b,c}$ (MeV)
Tungsten (W)	0.057	0.059	0.067	0.069	0.012

Table 4. Gold (Au) x-ray characteristic [31].

Material	K_{a1} (MeV)	K_{a2} (MeV)	K_{b1} (MeV)	L_a (MeV)	L_b (MeV)	L_c (MeV)
Gold (Au)	0.068	0.066	0.077	0.012	0.011	0.013

Table 5. Molybdenum (Mo) x-ray characteristic [31].

Material	K_a (MeV)	K_b (MeV)	$L_{a,b,c}$ (MeV)
Molybdenum (Mo)	0.017	0.019	0.002

Table 6. Rhodium (Rh) x-ray characteristic [31].

Material	K_a (MeV)	K_b (MeV)	$L_{a,b,c}$ (MeV)
Rhodium (Rh)	0.020	0.022	0.002

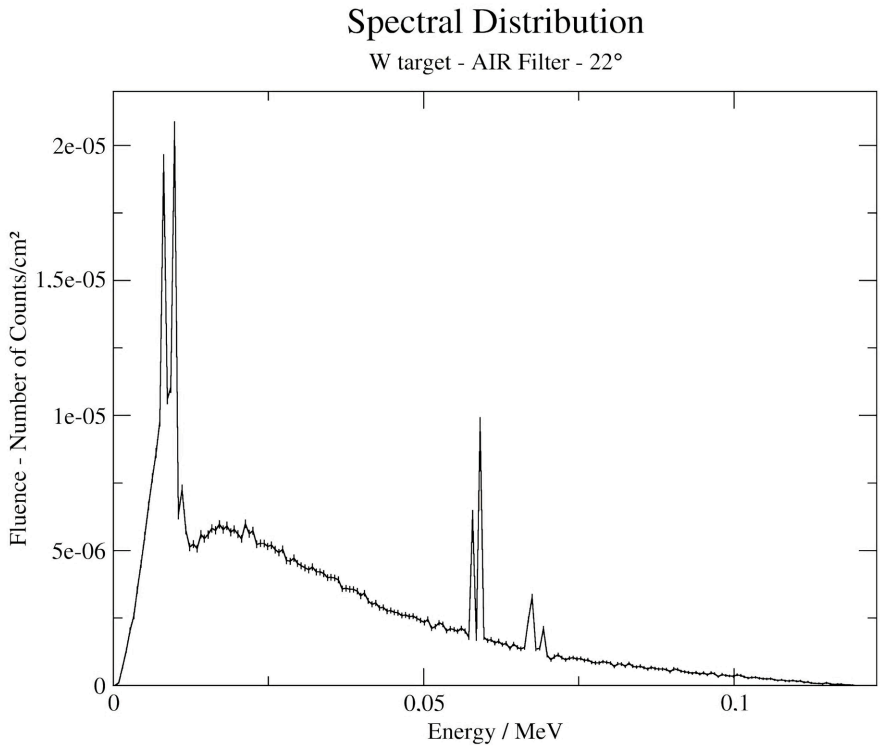

Figure 1. Tungsten (W) spectral distribution.

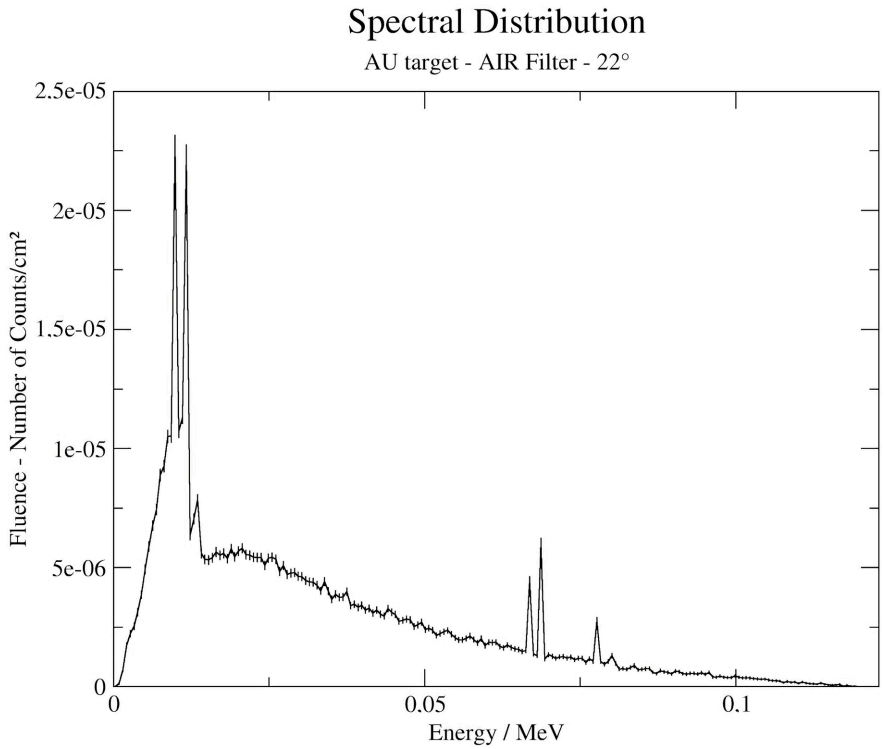

Figure 2. Gold (Au) spectral distribution.

of each anode-target material, produced from BEAMnrc, are presented with the theoretical values of **Tables 3-6**. This is a very important finding because it

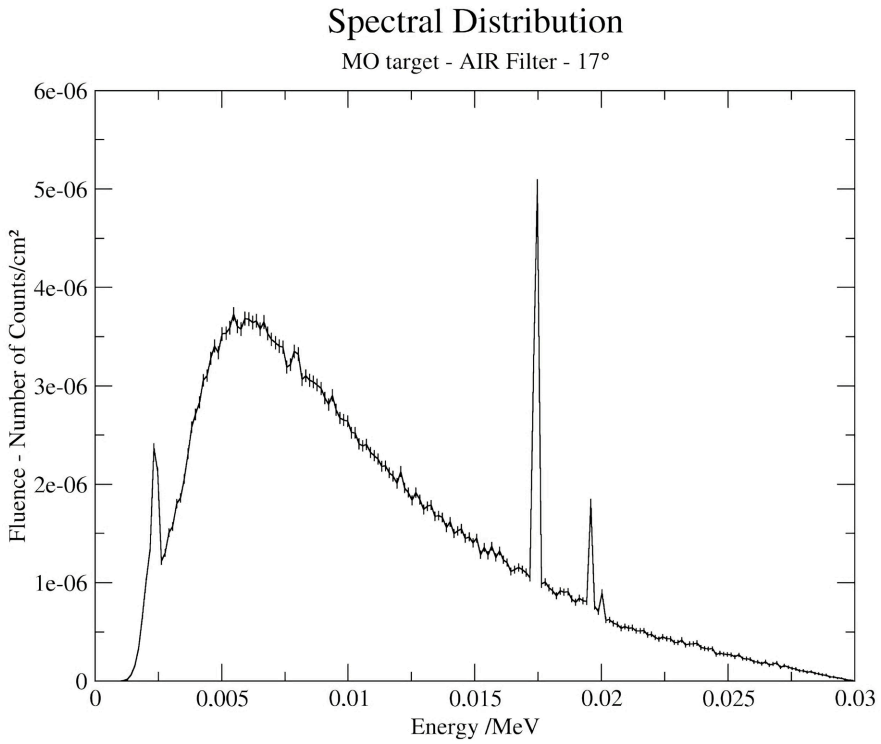

Figure 3. Molybdenum (Mo) spectral distribution.

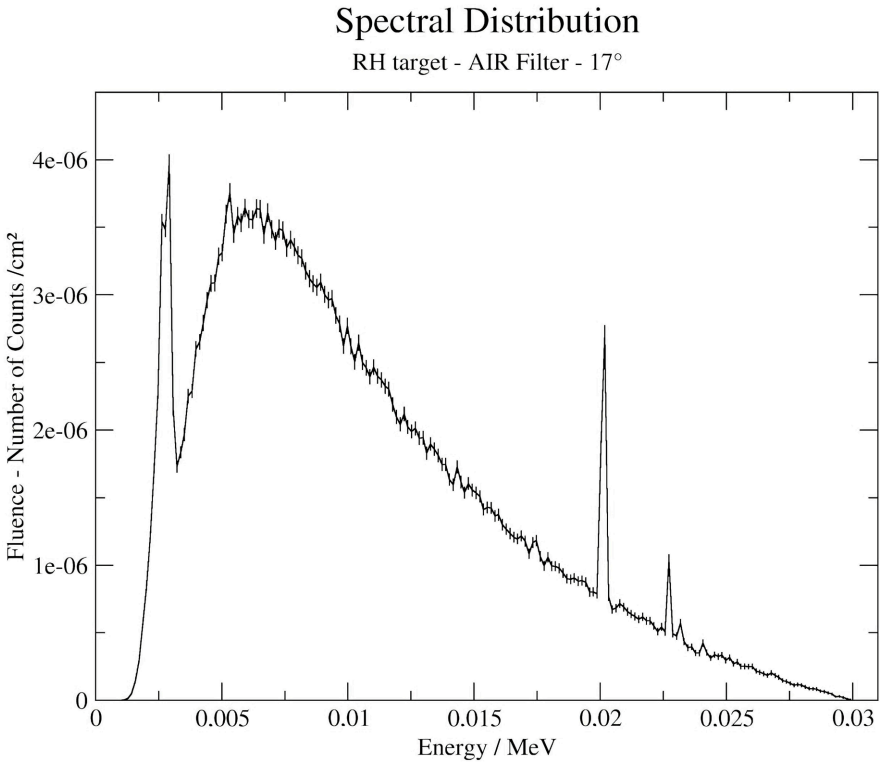

Figure 4. Rhodium (Rh) spectral distribution.

implies, in an additional way, that our simulation model is valid and that the Monte Carlo software is verified. More analytically in **Figure 1** we can see clearly

the K_{a1} = 0.057 MeV, K_{a2} = 0.059 MeV, K_{b1} = 0.067 MeV, K_{b2} = 0.069 MeV and $L_{a,b,c}$ = 0.012 MeV characteristic x-ray of the tungsten (W) target material. In **Figure 2** we can see clearly the K_{a1} = 0.068 MeV, K_{a2} = 0.066 MeV, K_{b1} = 0.077 MeV, L_a = 0.012 MeV, L_b = 0.011 MeV and L_c = 0.013 MeV characteristic x-ray of the gold (Au) anode-target material. The K_{a1}, K_{a2}, K_{b1}, K_{b2} are the ones that contribute to the image analysis and photon detection process of a CT scanner. In **Figure 3** we can see clearly the K_a = 0.017 MeV, K_b = 0.019 MeV and $L_{a,b,c}$ = 0.002 MeV, characteristic x-ray. In **Figure 4** we can clearly see the K_a = 0.020 MeV, K_b = 0.022 MeV and $L_{a,b,c}$ = 0.002 MeV characteristic x-ray. The K_a and K_b are the characteristic x-rays that penetrate the soft tissue and contribute to the mammographic procedure.

Furthermore, similarly with the works of Mesbahi *et al.* [12] and Kim *et al.* [13], which report the effect of anode angle using MCNP, **Figures 5-8** present comparable results, which are also derived by simulating a similar experimental design as the above publications. It may be observed that the anode angle has a noteworthy effect on the spectral distributions of each anode material. As shown in **Figures 5-8**, as the target's angle increases, a higher number of photons can hit the scoring plane, and the anode-target self-absorption (filtration) decreases, this phenomenon is known as the heel effect and we can clearly see that in the spectral distribution produced. This effect is more intense in the spectral distribution of **Figure 7** & **Figure 8**, for low energy photons, (30 keV photon energy). Based on the works of Verhaegen *et al.* [26] and Homolka *et al.* [9], **Figures 9-12** present clearly that the use of filters can significantly reduce an important amount of bremsstrahlung photons from the low energy band, allowing, hence, the electronics to achieve a better image during an examination. By filtering, a very large

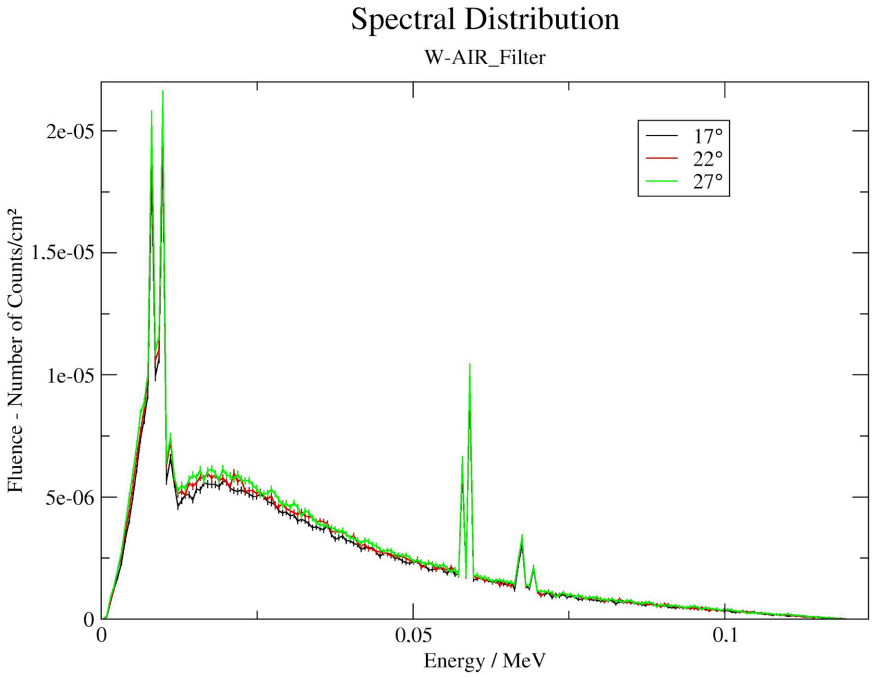

Figure 5. Tungsten (W) spectral distributions for angles 17˚ - 22˚ - 27˚.

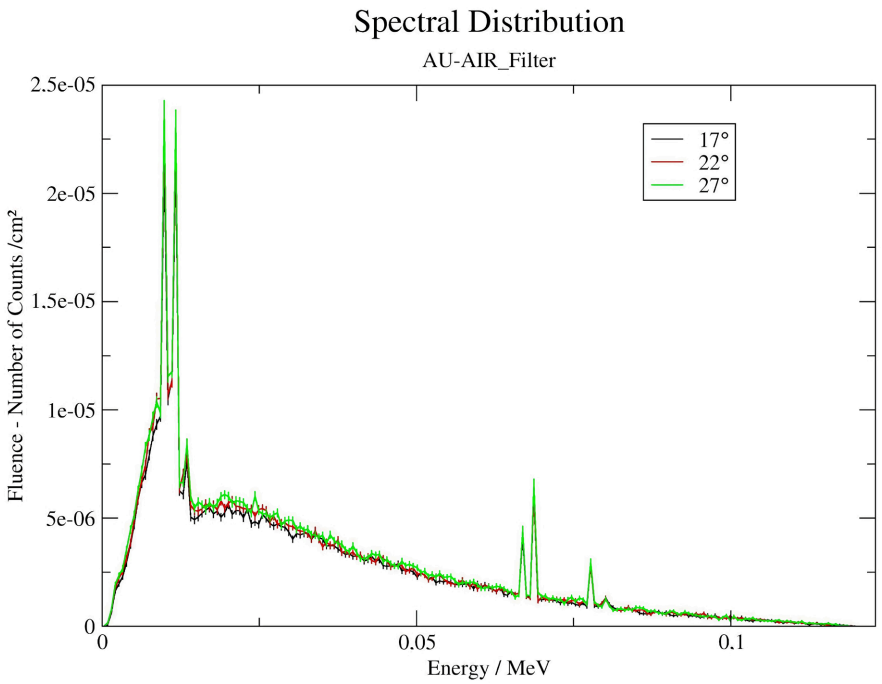

Figure 6. Gold (Au) spectral distributions for angles 17˚ - 22˚ - 27˚.

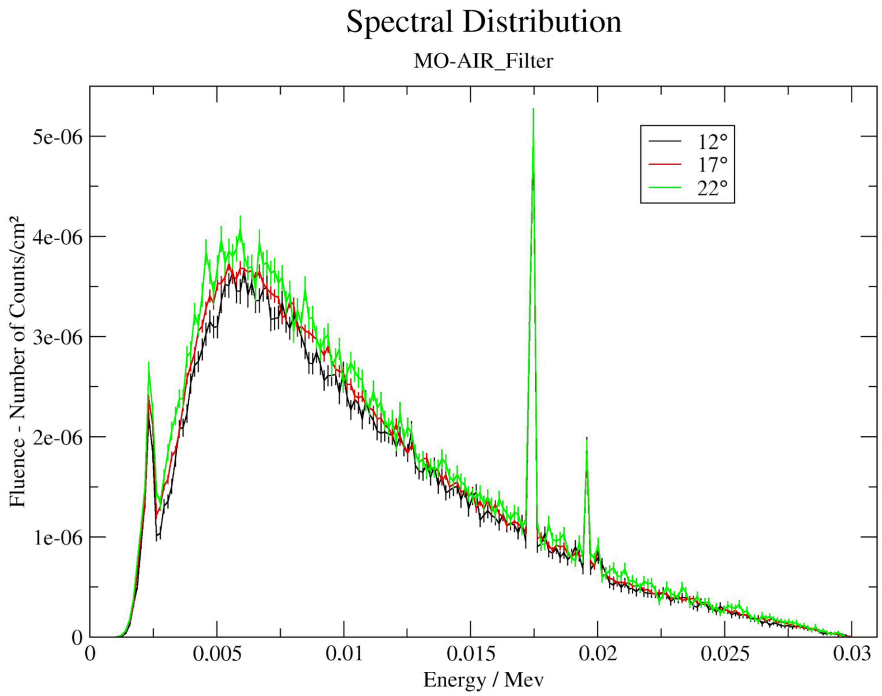

Figure 7. Molybdenum (Mo) spectral distributions for angles 12˚ - 17˚ - 22˚.

amount of those photons will not reach the patient and will not produce extra radiation thus, the exposure and the dose of the patients, are significantly decreased. More analytically in **Figure 9** we can see that the $L_{a,b,c}$ characteristics has been cut from the spectral distribution with the use of Al and with an extra Cu layer even more bremsstrahlung photons have been cut off but the K_{a1}, K_{a2}, K_{b1},

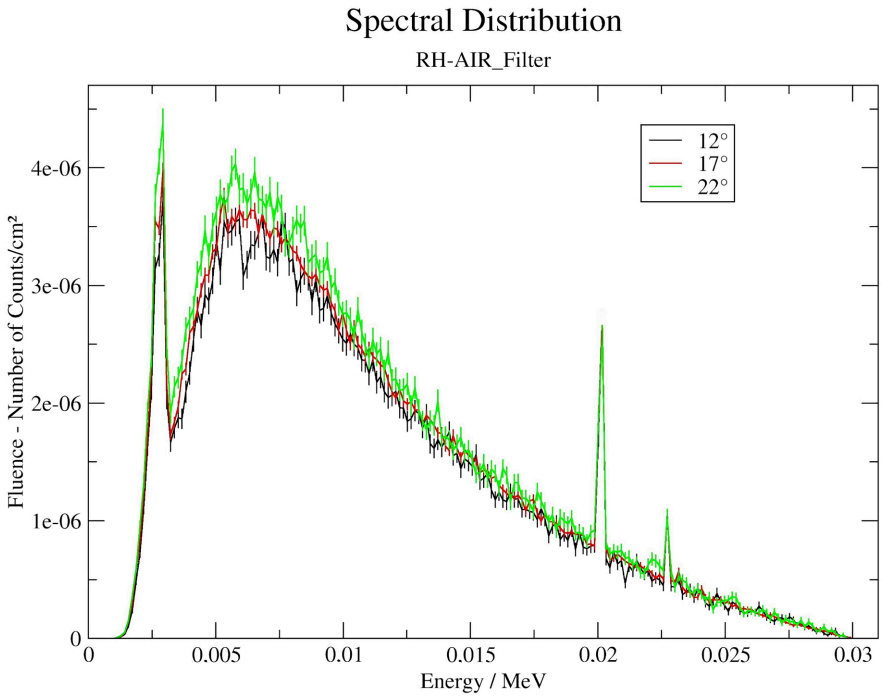

Figure 8. Rhodium (Rh) spectral distributions for angles 12˚ - 17˚ - 22˚.

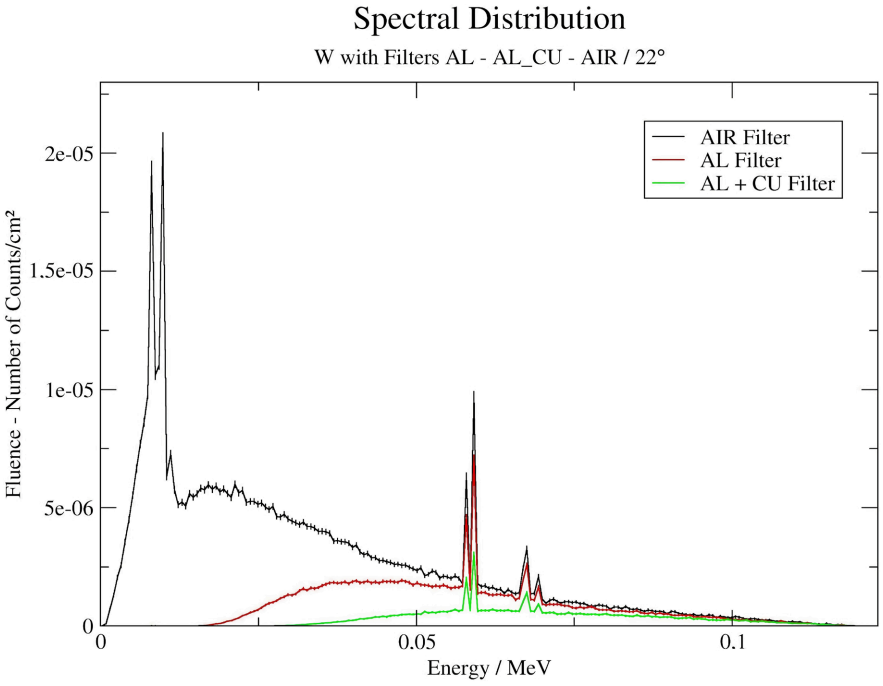

Figure 9. Tungsten (W) with angle 22˚ spectral distributions using filters of Air, Al, Al + Cu.

K_{b2}, have sustained. Also in **Figure 10** the same effect is taking place as the layers of Al and Cu have been applied the low energy bremsstrahlung photons don't pass to the patient, but only the K_{a1}, K_{a2}, K_{b1} are let through. The ideal situation would be for all the bremsstrahlung photons to cut off and only the K‹ characteristic

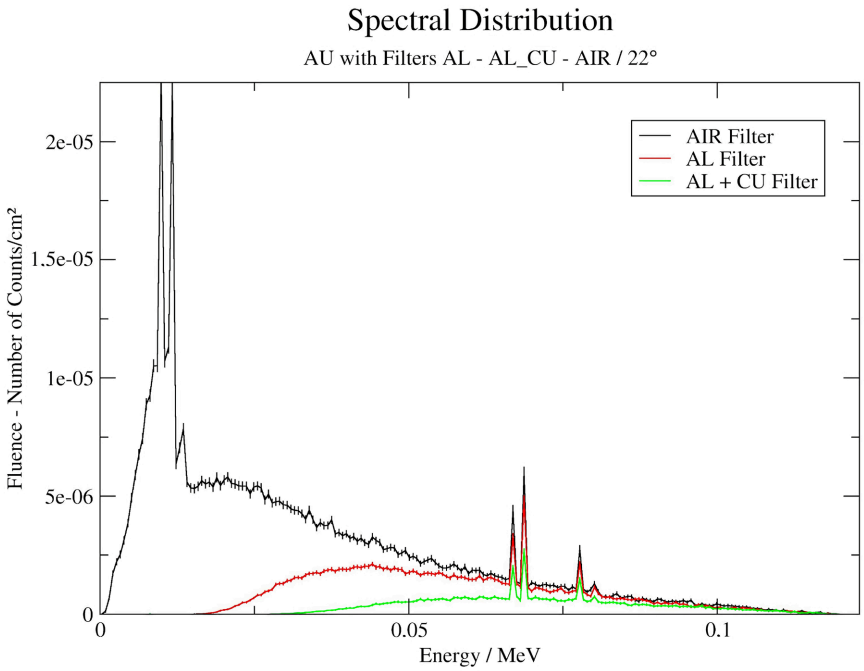

Figure 10. Gold (Au) with angle 22˚ spectral distributions using filters of Air, Al, Al + Cu.

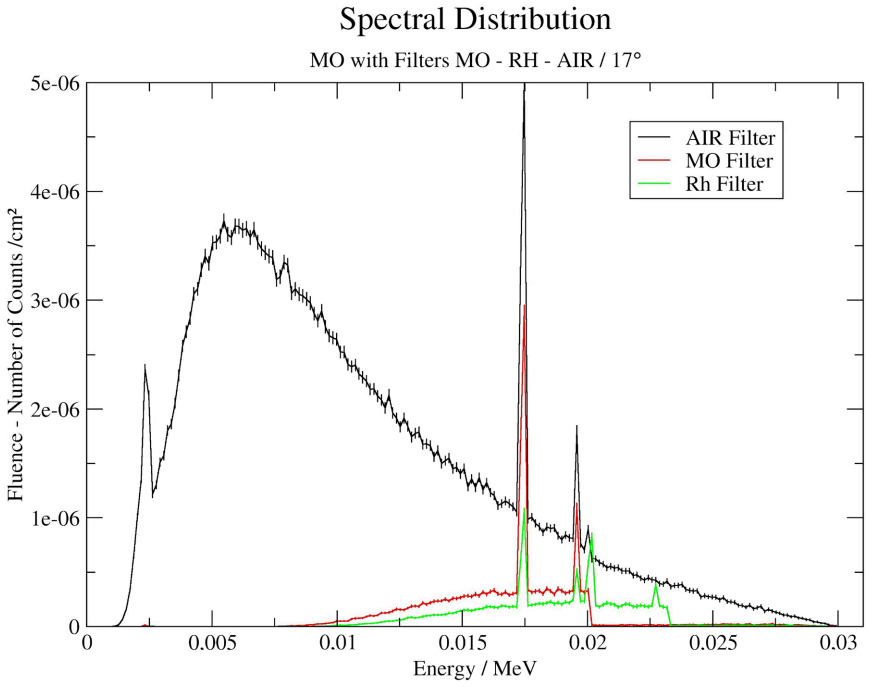

Figure 11. Molybdenum (Mo) with angle 17˚ spectral distributions using filters of Air, Mo, Rh.

x-rays to pass. In Figure 11 we can observe that with the application of Mo filter a large amount of photons has been cut off and only the K_a and K_b characteristics are let through, in most mammographic examinations Mo target with Mo filter are being applied but in recent years the application of Rh filter is being used as

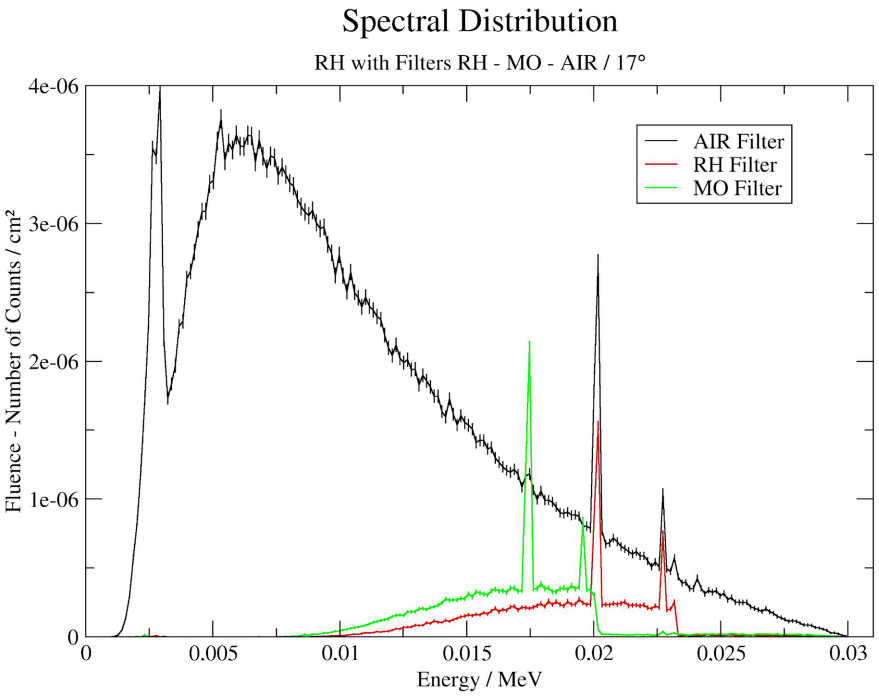

Figure 12. Rhodium (Rh) with angle 17˚ spectral distributions using filters of Air, Rh, Mo.

the intensity of the beam is lower but it lets other characteristics to be present. In Figure 12 we can observe the phenomena of lower energy photons to be cut-off letting only the K_a and K_b characteristic to pass, but in mammography only the Rh target with Rh filter is being used because if we apply Mo filtration the spectral distribution is being swift and the Mo filter is amplifying other characteristic x-ray production of the Rh target with increased intensity so this option is not ideal for the radiation exposure performance of the examination.

4. Conclusions

Because it's difficult to find the exact features of commercial x-ray tubes for medical imaging purposes, and the existing technology is not easily accessible, designing x-ray tubes with Monte Carlo methods is challenging. In this paper, we manage to utilize a simple but flexible approach. We examine a wide range of topics regarding x-ray tubes. We investigate the use of variance reduction and demonstrate its importance in Monte Carlo simulation, as it yields even to 20 - 30 times faster running time, at least for a certain scenario. Secondly, we validate our model via the BEAMnrc application for all employed anode-target materials, by comparing outcomes to those of similar works using different Monte Carlo software. With all our combinations of anode-target material and angles, we manage to investigate the effects of the anode's angle. We show that as the angle of the anode increases more photons are scored and this is a property connected to the heel effect and the self-absorption on the anode, we demonstrate these effects on the spectral distributions.

Lastly, we report that when photons are filtered in an examination, the dose of radiation received by a patient is significantly reduced. The findings obtained using our approach are comparable to the outcomes of recent studies.

After taking into consideration the theory and previous works on the subject of generation and creation of x-rays for medical imaging equipment we can support the view that BEAMnrc is a software that can be used to investigate efficiently and effectively x-ray tubes, as it is comparable to other commercial software, while it imposes great advantages.

Acknowledgements

The work of authors at the University of West Attica has been funded by The Special Account for Research Funds of ELKE/PADA.

Conflicts of Interest

There are no conflicts of interest revealed by the manuscript's writers.

References

[1] Li, X., Samei, E., Segars, W.P., Sturgeon, M.G., Colsher, G.J., Toncheva, G., Yoshizumi, T.T., *et al.* (2011) Patient-Specific Radiation Dose and Cancer Risk Estimation in CT: Part I. Development and Validation of a Monte Carlo Program. *Medical Physics*, **38**, 397-407. https://doi.org/10.1118/1.3515839

[2] Omar, A., Bujila, R., Fransson, A., Andreo, P. and Poludniowski, G. (2016) A Framework for Organ Dose Estimation in X-Ray Angiography and Interventional Radiology Based on Dose-Related Data in DICOM Structured Reports. *Physics in Medicine and Biology*, **61**, 3063-3038. https://doi.org/10.1088/0031-9155/61/8/3063

[3] Muller, M. and Hendriks, B.H.W. (2013) Recovering Intrinsic fluorescence by Monte Carlo Modeling. *Journal of Biomedical Optics*, **18**, Article ID: 027009. https://doi.org/10.1117/1.JBO.18.2.027009

[4] Ay, M.R., Sarkar, S., Shahriari, M., Sardari, D. and Zaidi, H. (2005) Assessment of Different Computational Models for Generation of X-Ray Spectra in Diagnostic Radiology and Mammography. *Medical Physics*, **32**, 1660-1675. https://doi.org/10.1118/1.1906126

[5] Tennant, M. and Kruger, E. (2013) A Dental Public Health Approach Based on Computational Mathematics: Monte Carlo Simulation of Childhood Dental Decay. *International Dental Journal*, **63**, 39-42. https://doi.org/10.1111/idj.12003

[6] Andreo, P. (2018) Monte Carlo Simulations in Radiotherapy Dosimetry. *Radiation Oncology*, **13**, Article No. 121. https://doi.org/10.1186/s13014-018-1065-3

[7] Salehi, Z., Ali, Y.N.K. and Yusoff, A.L. (2012) X-Ray Spectra and Quality Parameters from Monte Carlo Simulation and Analytical Filters. *Applied Radiation and Isotopes*, **70**, 2586-2589. https://doi.org/10.1016/j.apradiso.2011.12.007

[8] Adeli, R., Shirmardi, S.P., Amiri, J., Singh, V.P. and Medhat, M.E. (2015) Simulation and Comparison of Radiology X-Ray Spectra by MCNP and GEANT4 Codes. *Journal of Paramedical Sciences* (*JPS*), **6**, 8-14.

[9] Homolka, P. and Figl, M. (2018) Equivalent Thicknesses of Beam Hardening Filters Consisting of Aluminum, Copper, Al/Cu and Al/Gold Combinations and Plumbiferous Acrylic for 40 to 150 kVp Diagnostic Spectra. *Journal of Radiological Protec-*

tion, **38**, 1269-1283. https://doi.org/10.1088/1361-6498/aadaf4

[10] Cheng, Y., Zhang, J., Lee, Y.Z., Gao, B., Dike, S., Lin, W., Lu, J.P., *et al.* (2004) Dynamic Radiography Using a Carbon-Nanotube-Based Field-Emission X-Ray Source. *Review of Scientific Instruments*, **75**, 3264-3267. https://doi.org/10.1063/1.1791313

[11] Knoll, G.F. (2010) Radiation Detection and Measurement. 4th Edition, John Wiley & Sons Inc., Hoboken.

[12] Mesbahia, A. and Zakariaee, S.S. (2013) Effect of Anode Angle on Photon Beam Spectra and Depth Dose Characteristics for X-RAD320 Orthovoltage Unit. *Reports of Practical Oncology & Radiotherapy*, **18**, 148-152. https://doi.org/10.1016/j.rpor.2012.12.001

[13] Kim, G. and Lee, R. (2016) Effect of Target Angle and Thickness on the Heel Effect and X-Ray Intensity Characteristics for 70 kV X-Ray Tube Target. *Progress in Medical Physics*, **27**, 272-276. https://doi.org/10.14316/pmp.2016.27.4.272

[14] Burgess, A.E. (1985) Physical Measurements of Heavy Metal Filter Performance. *Medical Physics*, **12**, 225-231. https://doi.org/10.1118/1.595709

[15] Siedband, M.P. (1987) Beam Filtration in Diagnostic Radiology. In: Garrett, D.A. and Brachem, D.A., Eds., *Real-Time Radiologic Imaging: Medical and Industrial Applications*, American Society for Testing and Materials, West Conshohocken, 156-167. https://doi.org/10.1520/STP27505S

[16] Brenner, D.J. and Amols, H.I. (1989) Enhanced Risk from Low-Energy Screen-Film Mammography X-Rays. *The British Journal of Radiology*, **62**, 910-914. https://doi.org/10.1259/0007-1285-62-742-910

[17] Ay, M.R., Shahriari, M., Sarkar, S., Adib, M. and Zaidi, H. (2004) Monte Carlo Simulation of X-Ray Spectra in Diagnostic Radiology and Mammography Using MCNP4C. *Physics in Medicine and Biology*, **49**, 4897-4917. https://doi.org/10.1088/0031-9155/49/21/004

[18] Salvat, F., Fernandez-Varea, J.M., Sempau, J. and Llovet, X. (2006) Monte Carlo Simulation of Bremsstrahlung Emission by Electrons. *Radiation Physics and Chemistry*, **75**, 1201-1219. https://doi.org/10.1016/j.radphyschem.2005.05.008

[19] Bote, D., Llovet, X. and Salvat, F. (2008) Monte Carlo Simulation of Characteristic X-Ray Emission from Thick Samples Bombarded by Kiloelectronvolt Electrons. *Journal of Physics D: Applied Physics*, **41**, Article ID: 105304. https://doi.org/10.1088/0022-3727/41/10/105304

[20] Maged, M., Chakir, E., Boukhal, H., Saeed, M. and Bardouni, T.E. (2016) Evaluation of Variance Reduction Techniques in BEAMnrc Monte Carlo Simulation to Improve the Computing Efficiency. *Journal of Radiation Research and Applied Sciences*, **9**, 424-430. https://doi.org/10.1016/j.jrras.2016.05.005

[21] Bootsma, G.J., Nordstrom, H., Eriksson, M. and Jaffray, D.A. (2020) Monte Carlo kilovoltage X-Ray Tube Simulation: A Statistical Analysis and Compact Simulation Method. *Physica Medica*, **72**, 80-87. https://doi.org/10.1016/j.ejmp.2020.03.015

[22] Hjorringgaard, G.J., Ankjaergaard, C., Bailey, M. and Miller, A. (2020) Alanine Pellet Dosimeter Efficiency in a 40 kV X-Ray Beam Relative to Cobalt-60. *Radiation Measurements*, **136**, Article ID: 106374. https://doi.org/10.1016/j.radmeas.2020.106374

[23] Rogers, D.W.O., Walters, B. and Kawrakow, I. (2021) BEAMnrc Users Manual. NRCC Report PIRS-0509(A), National Research Council of Canada.

[24] Kawrakow, I., Rogers, D.W.O. and Walters, B. (2004) Large Efficiency Improvements in BEAMnrc Using Directional Bremsstrahlung Splitting. *Medical Physics*,

31, 2883-2898. https://doi.org/10.1118/1.1788912

[25] Dance, D.R. (2014) Diagnostic Radiology Physics. IAEA, Vienna.

[26] Verhaegen, F. and Castellano, I.A. (2002) Microdosimetric Characterisation of 28 KVp Mo/Mo, Rh/Rh, Rh/Al, W/Rh and Mo/Rh Mammography X Ray Spectra. *Radiation Protection Dosimetry*, **99**, 393-396. https://doi.org/10.1093/oxfordjournals.rpd.a006816

[27] Omar, A., Andreo, P. and Poludniowski, G. (2018) A Model for the Emission of K and L X Rays from an X-Ray Tube. *Nuclear Instruments and Methods in Physics Research Section B: Beam Interactions with Materials and Matter*, **437**, 36-47. https://doi.org/10.1016/j.nimb.2018.10.026

[28] Shi, C. and Wang, B. (2017) Preliminary Monte Carlo Investigation of Using Ir-192 as the Source for Real Time Imaging Purpose. *International Journal of Medical Physics, Clinical Engineering and Radiation Oncology*, **6**, 21-30. https://doi.org/10.4236/ijmpcero.2017.61003

[29] Ma, C.M. and Rogers, D.W. (2012) BEAMDP Users Manual. NRCC Report PIRS-0509(C), National Research Council of Canada.

[30] Brinkert, T. (2015) Grace User's Guide (for Grace-5.1.25). Semibyte Srls, Provincia di Prato.

[31] Thompson, C.A., Kirz, J., Attwood, T.D., Gullikson, M.E., Liu, Y., *et al.* (2009) X-Ray Data Booklet. 3rd Edition, Lawrence Berkeley National Laboratory, Berkeley, CA.